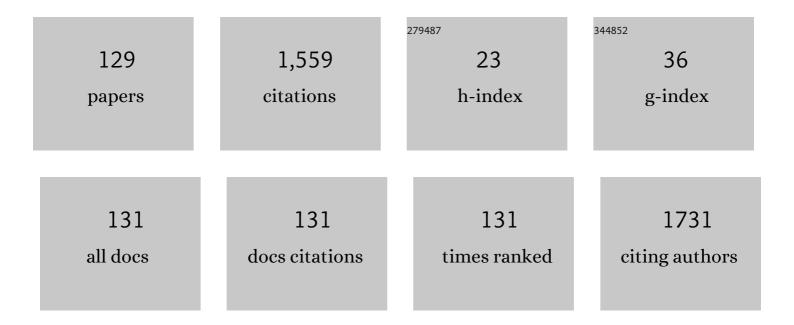
## Na Chen

## List of Publications by Year in descending order

Source: https://exaly.com/author-pdf/2413610/publications.pdf Version: 2024-02-01



#	Article	IF	CITATIONS
1	Highly Sensitive Liquid-Level Sensor Based on Etched Fiber Bragg Grating. IEEE Photonics Technology Letters, 2007, 19, 1747-1749.	1.3	158
2	Passively Q-switched erbium-doped fiber laser using evanescent field interaction with gold-nanosphere based saturable absorber. Optics Express, 2014, 22, 18537.	1.7	76
3	In-Fiber Mach–Zehnder Interferometer Based on Double Cladding Fibers for Refractive Index Sensor. IEEE Sensors Journal, 2011, 11, 2395-2400.	2.4	65
4	Cladding mode resonances of etch-eroded fiber Bragg grating for ambient refractive index sensing. Applied Physics Letters, 2006, 88, 133902.	1.5	61
5	Surface-enhanced Raman spectroscopy of serum accurately detects prostate cancer in patients with prostate-specific antigen levels of 4–10 ng/mL. International Journal of Nanomedicine, 2017, Volume 12, 5399-5407.	3.3	56
6	Gold Nanoparticles-Modified Tapered Fiber Nanoprobe for Remote SERS Detection. IEEE Photonics Technology Letters, 2014, 26, 777-780.	1.3	53
7	A Fiber-Optic Sensor for Acoustic Emission Detection in a High Voltage Cable System. Sensors, 2016, 16, 2026.	2.1	49
8	Temperature sensor using an optical fiber coupler with a thin film. Applied Optics, 2008, 47, 3530.	2.1	48
9	Temperature-Insensitivity Bending Sensor Based on Cladding-Mode Resonance of Special Optical Fiber. IEEE Photonics Technology Letters, 2009, 21, 76-78.	1.3	48
10	Special optical fiber for temperature sensing based on cladding-mode resonance. Optics Express, 2008, 16, 12967.	1.7	47
11	A Fading-Discrimination Method for Distributed Vibration Sensor Using Coherent Detection of \$varphi \$ -OTDR. IEEE Photonics Technology Letters, 2016, 28, 2752-2755.	1.3	42
12	Theoretical and experimental study on etched fiber Bragg grating cladding mode resonances for ambient refractive index sensing. Journal of the Optical Society of America B: Optical Physics, 2007, 24, 439.	0.9	36
13	In-series double cladding fibers for simultaneous refractive index and temperature measurement. Optics Express, 2010, 18, 13072.	1.7	34
14	Radiation-induced photoluminescence enhancement of Bi/Al-codoped silica optical fibers via atomic layer deposition. Optics Express, 2015, 23, 29004.	1.7	33
15	Photoluminescence properties of Bi/Al-codoped silica optical fiber based on atomic layer deposition method. Applied Surface Science, 2015, 349, 287-291.	3.1	33
16	Temperature characteristics of silicon core optical fiber Fabry–Perot interferometer. Optics Letters, 2015, 40, 1362.	1.7	33
17	Evaluation of expressed prostatic secretion and serum using surface-enhanced Raman spectroscopy for the noninvasive detection of prostate cancer, a preliminary study. Nanomedicine: Nanotechnology, Biology, and Medicine, 2017, 13, 1051-1059.	1.7	32
18	SERS detection of expired tetracycline hydrochloride with an optical fiber nano-probe. Analytical Methods, 2015, 7, 1307-1312.	1.3	30

#	Article	IF	CITATIONS
19	Deep convolutional neural networks combine Raman spectral signature of serum for prostate cancer bone metastases screening. Nanomedicine: Nanotechnology, Biology, and Medicine, 2020, 29, 102245.	1.7	29
20	Raman spectroscopy measurement of levofloxacin lactate in blood using an optical fiber nanoâ€probe. Journal of Raman Spectroscopy, 2015, 46, 197-201.	1.2	28
21	Fabrication of Ag/Au core-shell nanowire as a SERS substrate. Optical Materials, 2013, 35, 690-692.	1.7	25
22	Sapphire Fabry–Perot interferometer for high-temperature pressure sensing. Applied Optics, 2020, 59, 5189.	0.9	25
23	The Orbital Angular Momentum Fiber Modes for Magnetic Field Sensing. IEEE Photonics Technology Letters, 2019, 31, 893-896.	1.3	24
24	The image-based analysis and classification of urine sediments using a LeNet-5 neural network. Computer Methods in Biomechanics and Biomedical Engineering: Imaging and Visualization, 2020, 8, 109-114.	1.3	24
25	A Heterostructured Graphene Quantum Dots/β-Ga <sub>2</sub> O <sub>3</sub> Solar-Blind Photodetector with Enhanced Photoresponsivity. ACS Applied Materials & Interfaces, 2022, 14, 16846-16855.	4.0	22
26	Characterization of a high birefringence fibre Bragg grating sensor subjected to non-homogeneous transverse strain fields. Measurement Science and Technology, 2006, 17, 939-942.	1.4	21
27	CO <sub>2</sub> laser annealing of Ge core optical fibers with different laser power. Optical Materials Express, 2019, 9, 1333.	1.6	19
28	Quasi-Distributed IFPI Sensing System Demultiplexed With FFT-Based Wavelength Tracking Method. IEEE Sensors Journal, 2012, 12, 2875-2880.	2.4	18
29	SERS Taper-Fiber Nanoprobe Modified by Gold Nanoparticles Wrapped with Ultrathin Alumina Film by Atomic Layer Deposition. Sensors, 2017, 17, 467.	2.1	17
30	Cylindrical vector modes based Mach-Zehnder interferometer with vortex fiber for sensing applications. Applied Physics Letters, 2019, 115, .	1.5	17
31	Surface-enhanced Raman spectroscopy before radical prostatectomy predicts biochemical recurrence better than CAPRA-S. International Journal of Nanomedicine, 2019, Volume 14, 431-440.	3.3	17
32	Segmenting nailfold capillaries using an improved U-net network. Microvascular Research, 2020, 130, 104011.	1.1	17
33	Cascaded Mach-Zehnder interferometers in crystallized sapphire-derived fiber for temperature-insensitive filters. Optical Materials Express, 2017, 7, 1406.	1.6	16
34	3D Printing Technique-Improved Phase-Sensitive OTDR for Breakdown Discharge Detection of Gas-Insulated Switchgear. Sensors, 2020, 20, 1045.	2.1	16
35	Effects of distributed birefringence on fiber Bragg grating under non-uniform transverse load. Optics and Laser Technology, 2008, 40, 1037-1040.	2.2	14
36	Raman Spectroscopy Reveals Abnormal Changes in the Urine Composition of Prostate Cancer: An Application of an Intelligent Diagnostic Model with a Deep Learning Algorithm. Advanced Intelligent Systems, 2021, 3, 2000090.	3.3	13

#	Article	IF	CITATIONS
37	Cladding index modulated fiber grating. Optics Communications, 2006, 259, 587-591.	1.0	12
38	Surface-enhanced Raman scattering spectra revealing the inter-cultivar differences for Chinese ornamental Flos Chrysanthemum: a new promising method for plant taxonomy. Plant Methods, 2017, 13, 92.	1.9	12
39	Distributed Vibration Sensor With Laser Phase-Noise Immunity by Phase-Extraction φ-OTDR. Photonic Sensors, 2019, 9, 223-229.	2.5	12
40	Exceeding 50% slope efficiency DBR fiber laser based on a Yb-doped crystal-derived silica fiber with high gain per unit length. Optics Express, 2020, 28, 23771.	1.7	12
41	Use of Fiber Bragg Grating Sensors for Determination of a Simply Supported Rectangular Plane Plate Deformation. IEEE Photonics Technology Letters, 2007, 19, 1242-1244.	1.3	11
42	Four-wave mixing stability in hybrid photonic crystal fibers with two zero-dispersion wavelengths. Optics Express, 2013, 21, 30859.	1.7	10
43	Highly sensitive liquid level sensor based on etched fiber Bragg grating. Proceedings of SPIE, 2008, , .	0.8	9
44	In vivo Raman measurement of levofloxacin lactate in blood using a nanoparticle-coated optical fiber probe. Biomedical Optics Express, 2016, 7, 810.	1.5	9
45	All-Fiber Multiplexing and Transmission of High-Order Circularly Polarized Orbital Angular Momentum Modes With Mode Selective Couplers. IEEE Photonics Journal, 2019, 11, 1-9.	1.0	9
46	Distinguishing Cancerous Liver Cells Using Surface-Enhanced Raman Spectroscopy. Technology in Cancer Research and Treatment, 2016, 15, 36-43.	0.8	8
47	Sol–gel silica glass-cladding semiconductor-core optical fiber. Materials Today Communications, 2017, 11, 179-183.	0.9	8
48	LED Phototherapy with Gelatin Sponge Promotes Wound Healing in Mice. Photochemistry and Photobiology, 2018, 94, 179-185.	1.3	8
49	The study of ultrasound and iontophoresis on oxaprozin transdermal penetration using surface-enhanced Raman spectroscopy. Drug Delivery and Translational Research, 2020, 10, 83-92.	3.0	7
50	Cladding-mode resonance of a double-cladding fiber at a near modal cut-off wavelength for RI sensing. Measurement Science and Technology, 2010, 21, 094028.	1.4	6
51	Dynamic temperature monitoring and control with fully distributed fiber Bragg grating sensor. , 2010, , .		6
52	Fabrication of optical fiber sensor based on double-layer SU-8 diaphragm and the partial discharge detection. Optoelectronics Letters, 2015, 11, 61-64.	0.4	6
53	Few-mode ring-core quantum dots-doped optical fiber amplifier. Optical Fiber Technology, 2019, 51, 59-63.	1.4	6
54	Effects of annealing on the residual stresses distribution and the structural properties of Si core fiber. Optical Fiber Technology, 2018, 41, 193-199.	1.4	5

#	Article	IF	CITATIONS
55	The fabrication of a high-sensitivity surface-enhanced Raman spectra substrate using texturization and electroplating technology. Applied Surface Science, 2019, 490, 109-116.	3.1	5
56	Surface-enhanced Raman spectroscopy of preoperative serum samples predicts Gleason grade group upgrade in biopsy Gleason grade group 1 prostate cancer. Urologic Oncology: Seminars and Original Investigations, 2020, 38, 601.e1-601.e9.	0.8	5
57	Study of the Verdet constant of the holmium-doped silica fiber. OSA Continuum, 2020, 3, 1096.	1.8	5
58	Monitoring Junction Temperature of RF MOSFET under Its Working Condition Using Fiber Bragg Grating. Micromachines, 2022, 13, 463.	1.4	5
59	In vivo experiments of laser thermotherapy on liver tissue with FBG temperature distribution sensor. , 2012, , .		4
60	Fabrication and sensing characteristics of tilted long-period fiber gratings. , 2013, , .		4
61	Remote detection of the surface-enhanced Raman spectrum with the optical fiber nanoprobe. Optics and Spectroscopy (English Translation of Optika I Spektroskopiya), 2014, 116, 575-578.	0.2	4
62	Characteristics of cladding index modulated fiber gratings for ambient refractive index sensing. Optical Fiber Technology, 2009, 15, 90-94.	1.4	3
63	Fiber-optic intrinsic Fabry-Perot interferometric sensors fabricated by femtosecond lasers. , 2011, , .		3
64	Surface-enhanced Raman scattering sensor based on fused biconical taper zone of optical fiber. Journal of Shanghai University, 2011, 15, 26-30.	0.1	3
65	Fabrication of tilted long-period fiber gratings by CO2 laser. , 2011, , .		3
66	All-fiber power sensor based on silicon-germanium core fiber F-P cavity. Journal of Physics: Conference Series, 2017, 844, 012036.	0.3	3
67	PbS Quantum Dots Filled Photonic Crystal Fiber for All-fiber Amplifier. Journal of Physics: Conference Series, 2017, 844, 012060.	0.3	3
68	Laser stimulating ST36 with optical fiber induce blood component changes in mice: a Raman spectroscopy study. Journal of Biophotonics, 2018, 11, e201700262.	1.1	3
69	Composition and strain analysis of Si1-xGex core fiber with Raman spectroscopy. AIP Advances, 2018, 8, .	0.6	3
70	Thermal Poling of New Double-Hole Optical Fibers. Applied Sciences (Switzerland), 2019, 9, 2176.	1.3	3
71	Rapid and highâ€precision quantitative analysis based on substrate rotationâ€enhanced Raman scattering effect. Journal of Raman Spectroscopy, 2020, 51, 1278-1285.	1.2	3
72	A Micro-displacement Sensor Based on Cladding Mode Resonance of Optical Special Fiber. , 2008, , .		2

#	Article	IF	CITATIONS
73	Cladding Mode Resonance Based Fiber for Temperature Measurement. , 2008, , .		2
74	Fiber-optic refractive index sensor based on cladding-mode resonance. , 2009, , .		2
75	Raman scattering enhancement characteristic of Nb-doped silica fiber. Proceedings of SPIE, 2010, , .	0.8	2
76	Surface-enhanced Raman scattering optical fiber sensor using biconical taper fiber. , 2010, , .		2
77	The effect of laser acupuncture on hypoxia tolerance and inflammation reaction in mice with optical fiber acupuncture needle intra body. Journal of Innovative Optical Health Sciences, 2017, 10, 1650039.	0.5	2
78	Gold nanoparticles modified double-tapered fiber for SERS detection. Journal of Physics: Conference Series, 2017, 844, 012055.	0.3	2
79	Effect of controlling recrystallization from the melt on the residual stress and structural properties of the Silica-clad Ge core fiber. Optical Fiber Technology, 2017, 37, 6-10.	1.4	2
80	The dynamic process of laser drawing germanium core optical fiber. Journal of Physics: Conference Series, 2017, 844, 012058.	0.3	2
81	Ag Nanoparticles for the Direct Detection of Oxaprozin in the Blood Using Surface-Enhanced Raman Spectroscopy. ACS Applied Nano Materials, 2020, 3, 5928-5935.	2.4	2
82	Orbital Angular Momentum Optical Amplifier Based on PbS-Doped Ring-Core Fiber. Frontiers in Physics, 2020, 8, .	1.0	2
83	Monitoring the differentiation of dimethyl sulfoxideâ€induced human leukemia (HLâ€60) cells by Raman spectroscopy. Journal of Raman Spectroscopy, 2021, 52, 1086-1094.	1.2	2
84	Optical liquid level sensor based on cladding-mode resonance of specialty double-cladding fiber. , 2009, , .		2
85	Nailfold Microhemorrhage Segmentation with Modified U-Shape Convolutional Neural Network. Applied Sciences (Switzerland), 2022, 12, 5068.	1.3	2
86	Low-Loss Fiber-Optic Intrinsic Fabry-Perot Micro-Cavity Interferometric Sensor. , 2008, , .		1
87	Proposal for Second-Harmonic Generation Based on Mode Coupling in Coaxial Optical Fiber. IEEE Photonics Technology Letters, 2009, 21, 471-473.	1.3	1
88	In-fiber Michelson interferometer based on double-cladding fiber for refractive index sensing. Proceedings of SPIE, 2009, , .	0.8	1
89	A biconical taper multi-mode fiber SERS sensor. , 2010, , .		1
90	Dynamic analysis on the fabrication of CO <inf>2</inf> laser written long-period fiber gratings. , 2010, , .		1

#	Article	IF	CITATIONS
91	A biconical taper multi-mode fiber SERS sensor. , 2010, , .		1
92	Hepatocellular carcinoma cells Raman spectra with gold and silver colloid as SERS substrate. Proceedings of SPIE, 2011, , .	0.8	1
93	Preparation of gold colloid and its surface-enhanced Raman scattering properties. , 2011, , .		1
94	Change in refractive index of muscle tissue during laser-induced interstitial thermotherapy. Bio-Medical Materials and Engineering, 2014, 24, 807-813.	0.4	1
95	Carbon-coated magnetic particles increase tissue temperatures after laser irradiation. Journal of Innovative Optical Health Sciences, 2015, 08, 1550018.	0.5	1
96	Enhancing Laser Phase-noise Immunity of Distributed Vibration Sensor by Phase-extraction φ-OTDR. , 2018, , .		1
97	Excitation and Transmission of 12 OAM Modes in 3.7-km-long Ring Fiber with High Refractive Index Difference. , 2018, , .		1
98	A device designed for plant growth with automatic adjustment. , 2018, , .		1
99	Tapered optical fiber deposited with PbS as an optical fiber amplifier based on atomic layer deposition. Optical Engineering, 2018, 57, 1.	0.5	1
100	SERS Measurement Using Nanoprobe Tip with Laser-Induced Deposited Nanoparticles and Chemical Coated Nanoparticles. Journal of Nanoelectronics and Optoelectronics, 2017, 12, 201-204.	0.1	1
101	Fabry-Perot temperature sensor for quasi-distributed measurement utilizing OTDR. , 2008, , .		0
102	Fiber Bragg grating cladding mode resonance liquid-level sensor. , 2009, , .		0
103	Optical liquid level sensor based on cladding-mode resonance of specialty double-cladding fiber. , 2009, , .		0
104	Tapered optical fiber fabricated by high-frequency pulsed carbon dioxide laser. , 2010, , .		0
105	Fiber optic intrinsic Fabry-Perot temperature sensor fabricated by femtosecond lasers. , 2010, , .		0
106	Modified simulated annealing evolutionary algorithm for fully distributed fiber Bragg grating temperature sensing. Journal of Shanghai University, 2011, 15, 58-62.	0.1	0
107	Fabrication of fiber-optic EFPI with double-layer SU-8 diaphragm. Proceedings of SPIE, 2011, , .	0.8	0
108	Response of CO2 laser written long period fiber gratings packaged by polymer materials. Proceedings of SPIE, 2011, , .	0.8	0

Na Chen

#	Article	IF	CITATIONS
109	Gas furnace design for low-temperature and low-speed fiber drawing process. Proceedings of SPIE, 2011, , .	0.8	0
110	Surface-enhanced Raman scattering spectra of tomato epidermis on gold/ silver sol active substrate. Proceedings of SPIE, 2011, , .	0.8	0
111	A label-free antigen-antibody immunosensor based on a special double cladding fiber. Proceedings of SPIE, 2012, , .	0.8	0
112	SERS properties of gold core silver shell nanoparticles self-assembled on silica substrates and optical fiber endface. , 2012, , .		0
113	Interrogation of in-series double cladding fiber sensor for simultaneous refractive index and temperature measurement. , 2012, , .		0
114	Resonant optical nonlinearity of Nb-doped silica fiber measured with LPFG interferometer. , 2012, , .		0
115	Surface-enhanced Raman spectroscopy of mouse serum using silver colloid substrate. Proceedings of SPIE, 2012, , .	0.8	0
116	Characterization of Nb/Al codoped silica fiber by writing long-period gratings with CO2 laser. Optical Fiber Technology, 2013, 19, 519-522.	1.4	0
117	Fabry-Perot cavity based on sapphire-derived fiber for high temperature sensor. , 2015, , .		0
118	Laser-induced self-assembly gold nanoparticles on the silanized surface of a tapered fiber and its application as a SERS probe. Journal of Physics: Conference Series, 2017, 844, 012054.	0.3	0
119	Measurement and Imaging of Raman Spectroscopy with Nanoparticles. Frontiers in Nanobiomedical Research, 2017, , 23-37.	0.1	0
120	Strain Distribution in Silica-Clad Crystalline-Germanium-Core Fiber. Journal of Physics: Conference Series, 2017, 844, 012059.	0.3	0
121	Annealing Effcts on Luminescence Efficiency of Crystal Scintillation Optical Fiber for Radiotherapy. , 2018, , .		0
122	Generation of OAM Modes by Using Tapered Lensed Single Mode Fiber. , 2018, , .		0
123	The Raman spectroscopy measurement of interstitial fluid in ST36 acupoint by optical fiber probe. , 2018, , .		0
124	High Sensitivity Long-Period Fiber Gratings Written in Tapered Fibers by CO2 Laser. , 2012, , .		0
125	Oxidation detection of ascorbic acid using SERS. , 2014, , .		0
126	All-optical intensity modulation based on silicon core fiber. , 2015, , .		0

#	Article	IF	CITATIONS
127	The OAM transmission fiber based on step-index and graded-index refractive distribution. , 2019, , .		0
128	Accurate locating method in vibration sensing system based on φ-OTDR and 3D printing sensor. , 2019, , .		0
129	Permeation Effect Analysis of Drug Using Raman Spectroscopy for Iontophoresis. Applied Sciences (Switzerland), 2022, 12, 6871.	1.3	0